DFT Treatment of Hydrazine - Nitroform Interaction

Lemi Türker

Department of Chemistry, Middle East Technical University, Üniversiteler, Eskişehir Yolu No: 1, 06800 Çankaya/Ankara, Turkey; e-mail: lturker@gmail.com; lturker@metu.edu.tr

Abstract

In the present study, interaction of hydrazine and nitroform (trinitromethane) has been investigated via some models within the constraints of density functional theory at the level of B3LYP/6-311++G(d,p). The data have revealed that the electronic stability order of the models is 3>1>2>5>4 where model-3 is a cyclic one. The others are acyclic and some of them are ion-pair models. Some geometrical, physico chemical and quantum chemical data have been obtained and discussed. The results, overall, indicate that the interaction between the hydrazine and nitroform in the salt form is not ion-pair type, but the hydrogen of nitroform prefers to be linked to carbon atom, thus some sort of nonbonding interactions occur.

1. Introduction

Hydrazinium nitroformate (HNF) is an energetic oxidizer [1-3]. It is used to produce propellants which burn very rapidly, exhibiting very high combustion efficiency. Its high energy leads to propellants having high specific impulse. However, it is currently an expensive research chemical and available only in limited quantities. Another disadvantage of HNF is its limited thermal stability. However, hydrazinium nitroformate (hydrazine nitroform) is relatively resistant to shock, friction and percussion so that it is used extensively in production of high performance rocket propellants and gun propellants [4]. Other nitroformate energetic salts are also potential high-performance oxidizers which can be used in a solid propellant [5] and have attracted attention of various investigators [6-10].

HNF is a *salt* of hydrazine, a weak base and nitroform [NF] [2,4]. Trinitromethane (nitroform) and its salts have been known for almost more than a century and are the subject of several structure-related publications [11], including an *ab initio* study predicting a propeller-type structure for the anion (nitroformate) [12]. Xiao and coworkers investigated the intermolecular interaction of hydrazinium nitroformate ion pair using density functional theory [13].

The trinitromethane molecule, precursor of HNF has some interesting features. It can exist in two tautomeric forms; a nitroform (I) and an *aci*-form (II).

$$(O_2N)_3CH \rightleftharpoons (O_2N)_2C=NOOH$$

| I | II |
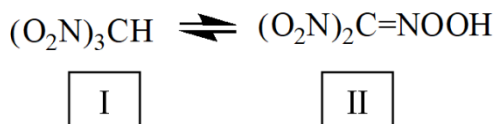
The colorless form (I) exists in solution acidified with HCl or H_2SO_4 and also in anhydrous benzene, CS_2 and ether [14]. Whereas, aqueous and basic solutions are intensely yellow colored which is due to the presence of *aci* tautomeric form (II). Although, its salts derive from the *aci* form (II), the silver and mercury salts exist in two forms: colorless and yellow. This would indicate that two forms of these salts, the nitro and *aci* can exist [14].

The three highly electron-withdrawing $-NO_2$ groups should make the hydrogen very positive. It is accordingly expected that $HC(NO_2)_3$ will be a strong acid, and indeed its experimentally determined pKa has been reported to equal 0.1 [14,15]. Although, nitro-*aci* tautomerism is expected, the *aci* tautomer of $HC(NO_2)_3$, formed by transfer of the proton to one of the nitro oxygens has not yet been isolated [16].

2. Method of Calculations

The geometry optimizations of all the structures leading to energy minima have been achieved first by using MM2 method which is followed by semi-empirical PM3 self consistent fields molecular orbital (SCF MO) method [17,18] at the restricted level [19,20]. Subsequent optimizations were achieved at Hartree-Fock level employing various basis sets. Then, geometry optimizations were managed within the framework of density functional theory [21,22] at the level of B3LYP/6-311++G(d,p) [19,23]. The exchange term of B3LYP consists of hybrid Hartree-Fock and local spin density (LSD) exchange functions with Becke's gradient correlation to LSD exchange [22,24]. The correlation term of B3LYP consists of the Vosko, Wilk, Nusair (VWN3) local correlation

functional [25] and Lee, Yang, Parr (LYP) correlation correction functional [26]. Also, vibrational analyses have been done on the optimized structures. The total electronic energies are corrected for the zero point vibrational energy (ZPE). Moreover, the normal mode analysis for each structure yielded no imaginary frequencies for the $3N–6$ vibrational degrees of freedom, where N stands for the number of atoms in the system. This has indicated that the structure of each molecule corresponds to at least a local minimum on the potential energy surface. All these calculations have been done by using the Spartan 06 package program [27].

3. Results and Discussion

Figure 1 shows the optimized structures and directions of the calculated dipole moment vectors of the models considered. Note that in all the cases tail of the dipole moment vector originates from the hydrazine moiety. Model-1 stands for the composite system of hydrazine and nitroform where the prevailing interactions should be the nonbonding ones. Whereas, model-2 stands for hydrazinium nitroformate ion pair.
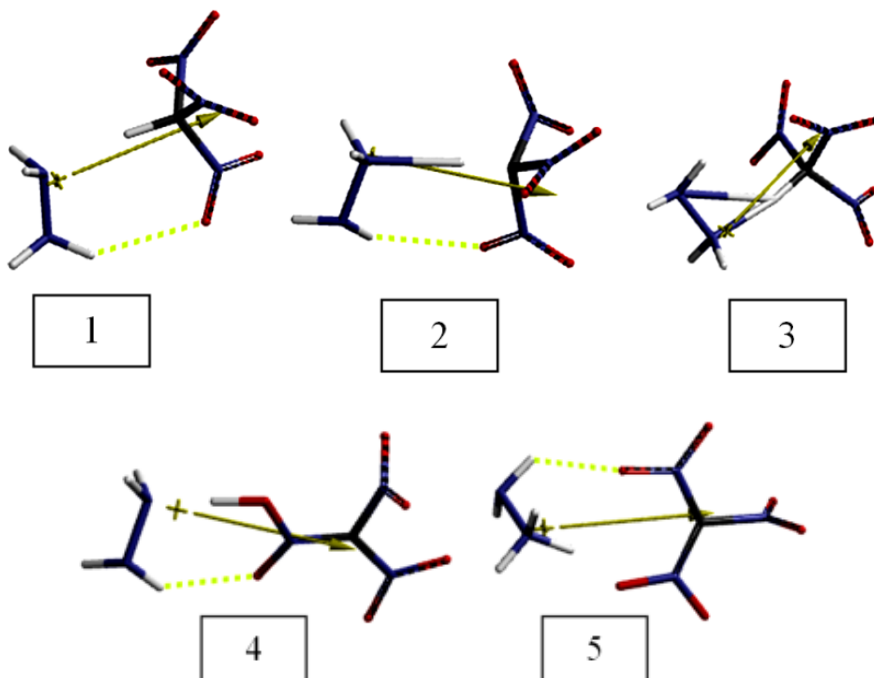

Figure 1. Optimized structures of the models considered (Hydrogen bonds shown as dashed lines).

Model-3 represents a nonclassical bonding in which the hydrogen binds to two nitrogen atoms of hydrazine and the carbon atom of nitroform. Model-4 shows the interaction between hydrazine and *aci* tautomer of nitroform. Model-5 is the ion pair formed between hydrazinium cation and the anion of the *aci* tautomer of nitroform (hydrazinium nitroformate from the *aci* tautomer). Note that in models 1-3 components, originating from nitroform, more or less preserve the nitroform geometry.

Figure 2 shows the calculated bond lengths in the models considered. The hydrazine components in model-1 and model-2 have one elongated N-H bond (1.81 and 1.98 Å, respectively). The C-H bond of nitroform in model-1 is 1.10 Å. In model-2, the nitroform hydrogen was initially linked to hydrazine component but after the optimization the distance from the same hydrogen atom to nitroformate carbon atom is just 1.10 Å which is a typical C-H bond length. Model-3, in which the hydrogen seems to linked to three
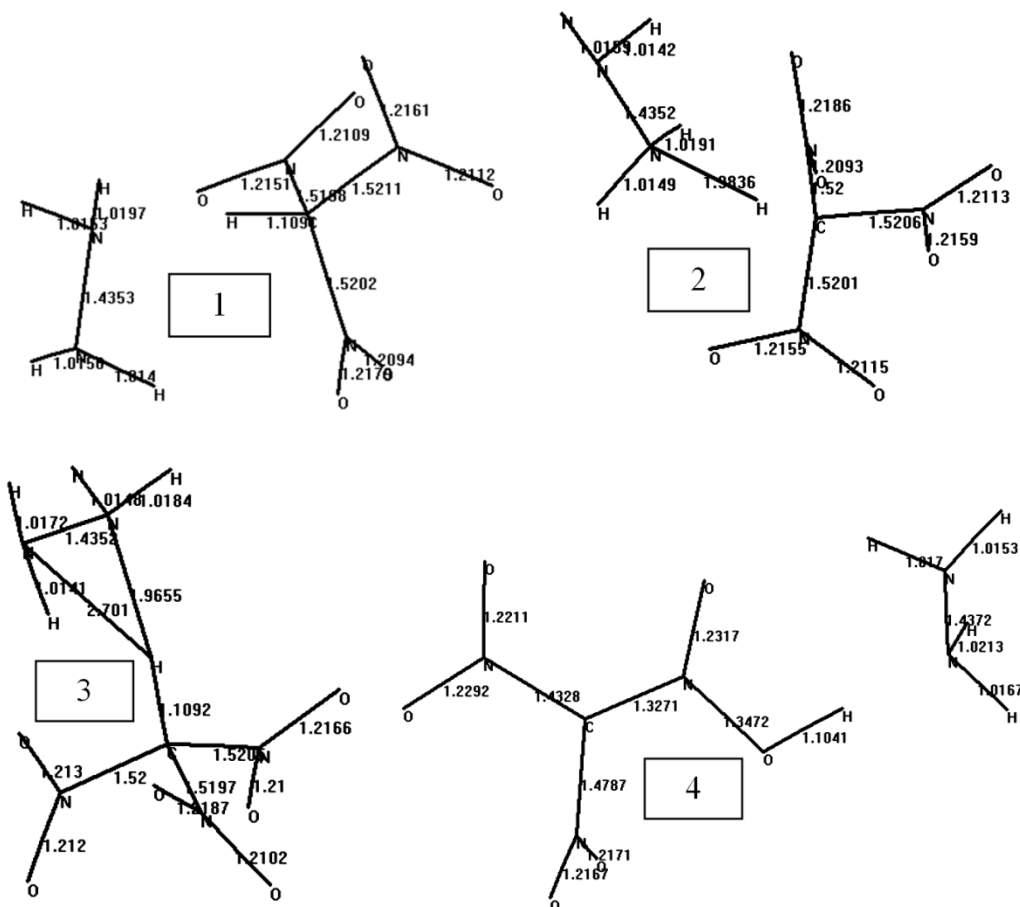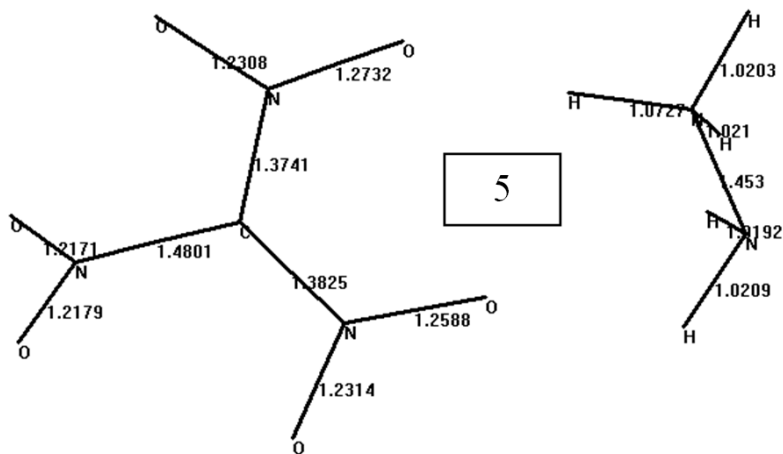
Figure 2. Calculated bond lengths (Å) in the models considered.

centers, has N-H linkages having lengths of 2.70 Å and 1.96 Å and C-H linkage of 1.10 Å. Thus, model-3 as model-2 prefers C-H rather than N-H bonding for the nitroform hydrogen. In the other models nitroform hydrogen linked to oxygen atom (model-4, *aci* tautomer of nitroform) or to hydrazine (model-5, an ion-pair from the *aci* tautomer), all having appropriate O-H or N-H bond lengths. Note that the C-H bond lengths in model-3 and model-1 are the same as 1.109 Å.

Table 1 shows some energies of the isomeric structures considered where E, ZPE and E_C stand for the total electronic energy, zero point vibrational energy and the corrected total electronic energy, respectively. The data in the table indicate that the stability order of the models is 3>1>2>5>4. In model-3, nitroform hydrogen is under the influence of both of the nitrogen atoms of hydrazine molecule, however the N-H bond lengths are unequal and N-N bond length (1.435 Å) in the hydrazine molecule which is not much different from the respective lengths in the other models. Note that models 4 and 5 are rather less stable than models 1-3 because in the optimized forms of them nitroform hydrogen is either structurally linked to different atoms or charge separation has occurred and not in the proximity of nitroform carbon. So, those models have higher electronic energies compared to the respective values of models 1-3.

Table 1. Some energies of the models considered.

| Models	E	ZPE	E_C
1	-2011369.51	286.53	-2011082.98
2	-2011369.44	286.63	-2011082.81
3	-2011370.74	286.87	-2011083.87
4	-2011345.37	282.64	-2011062.73
5	-2011354.48	291.17	-2011063.31

Energies in kJ/mol.

Table 2 shows dipole moment components and total value of the dipole moment for the models considered. The order for the dipole moments is 5>4>3>2>1. The order mostly should be dictated by the various possibilities of hydrogen bondings. Note that in reference 5 the weak interaction for cation and anion is attributed to vdW interaction but no H-bonds [5].

Table 2. Dipole moment components and the total value for the models considered.

| Models	X	Y	Z	Total
1	-0.047488	5.196565	0.996521	5.291464
2	-2.359477	4.740344	0.552835	5.323873
3	-0.376478	5.426420	0.234077	5.444498
4	8.984604	1.155886	-2.391708	9.369069
5	10.495689	2.795942	-1.589063	10.977336

In debye units.

Figure 3 shows the electrostatic potential (ESP) charges on the atoms of models 1-3 considered. Note that the ESP charges are obtained by the program based on a numerical method that generates charges that reproduce the electrostatic potential field from the entire wavefunction [27]. The figure shows that in the models carbon of the nitroform moiety has partial negative charge (-0.30 to -0.35) whereas the hydrogen originating from the nitroform has minute negative partial charge in models 1 and 3 but a minute positive partial charge in model-2.
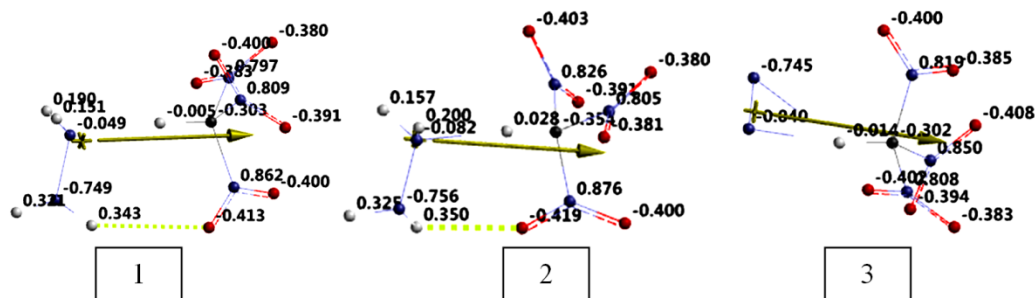
Figure 3. The ESP charges on atoms of models 1- 3 considered (Some hydrogen atoms not shown for clarity).

Figure 4 shows the electrostatic potential field maps of the models considered.
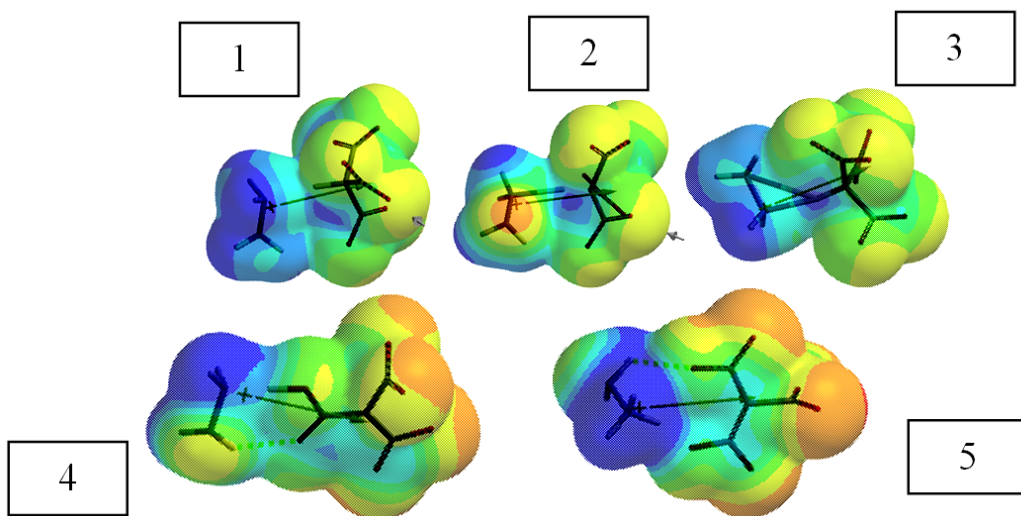
Figure 4. Electrostatic potential field maps of the models considered.

Table 3 shows some standard thermodynamic properties of the models considered. According to the data in the table, the order of 3>1>2>4>5 stands for H° (the exothermicity) of the models. The same order holds for G° values indicating that thermodynamically model-3 and model-5 are the most and the least favored ones, respectively. Of course many structural and electrical factors are influential on these orders.

Table 3. Some standard thermodynamic properties of the models considered.

Models	Hº (kJ/mol)	Sº (J/molº)	Gº (kJ/mol)
1	-2011071.047	428.88	-2011198.918
2	-2011070.882	428.59	-2011198.666
3	-2011071.956	427.73	-2011199.488
4	-2011051.277	423.80	-2011177.633
5	-2011051.739	424.46	-2011178.292

Table 4 lists various properties of the models considered. The area and volumes of the models follow the order of 1>2>3>4>5. The ovalites of the first three models are the same as well as the polarizability values.

Table 4. Various properties of the models considered.

Models	Area (Å^2)	Volume (Å^3)	Ovality	Polarizability	Log P
1	186.45	133.74	1.47	51.25	0.49
2	186.12	133.72	1.47	51.25	-
3	185.43	133.62	1.47	51.25	-
4	179.62	132.01	1.43	51.03	-0.43
5	176.09	131.56	1.41	51.07	-

Polarizability values in units of 10^{-30} m^3.

Figure 5 shows some of the molecular orbital energy levels of the models considered. The HOMO, LUMO energies and the interfrontier molecular orbital energy gaps, Δε, of the models are listed in Table 5.
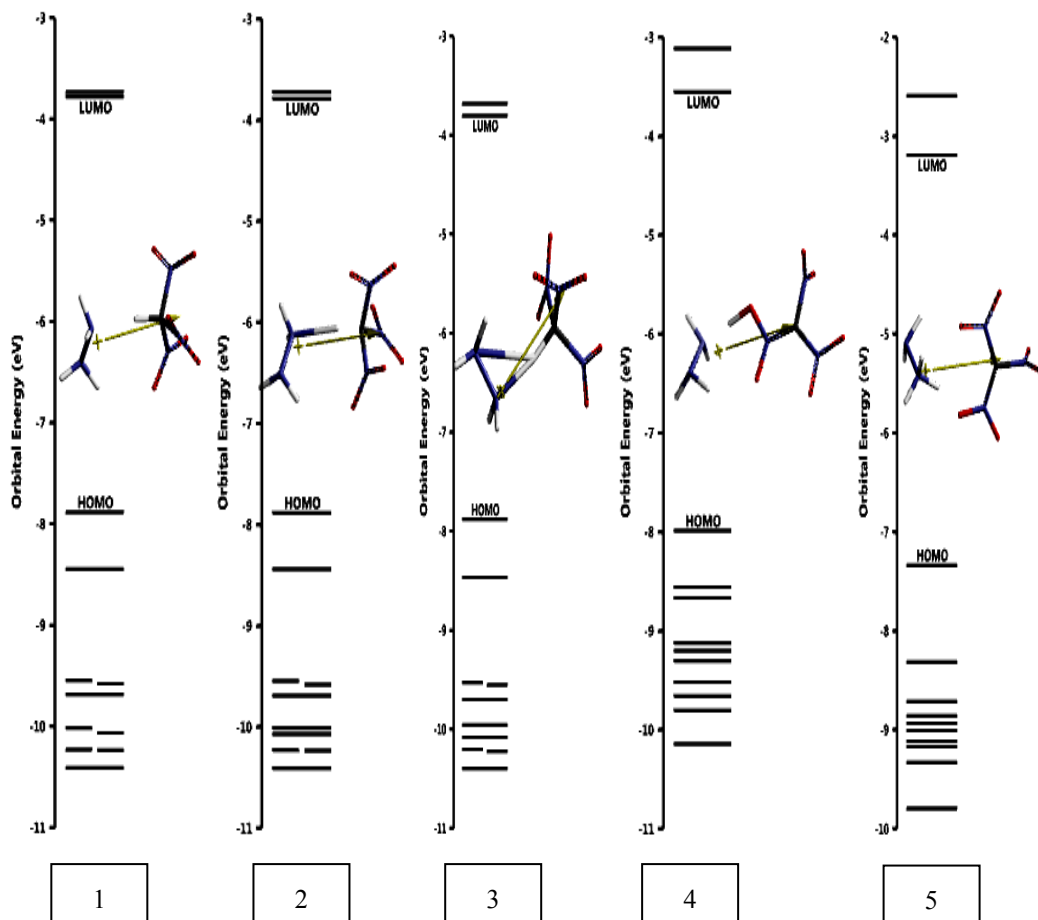
Figure 5. Some of the molecular orbital energy levels of the models considered.

As seen in Table 5, the HOMO and LUMO orders are 4<1<2<3<5 and 3<2<1<4<5, respectively. Consequently, the interfrontier molecular orbital energy gap $\Delta\varepsilon$ ($\Delta\varepsilon = \varepsilon_{LUMO} - \varepsilon_{HOMO}$) values of the models follows the order of 5>4>1>2>3. As compared to the respective energies of nitroform and hydrazine it is evident that the HOMO energies of the models are higher than nitroform but lower than hydrazine. It is also true for the LUMO energies. All these indicate the presence of some interaction between nitroform and hydrazine. However, the nature of interaction, in the light of the models and the related data harvested from them, indicate that the bonding is not covalent but a kind of electrostatic interaction as previously pointed out [5].

Table 5. The HOMO, LUMO energies and the interfrontier molecular orbital energy gaps ($\Delta\varepsilon$) of the models.

| Model	HOMO	LUMO	$\Delta\varepsilon$
1	-760.92	-365.06	395.86
2	-760.65	-365.60	395.05
3	-760.63	-367.14	393.49
4	-770.75	-342.95	427.80
5	-707.71	-308.09	399.62
Nitroform	-961.03	-399.35	561.68
Hydrazine	-566.17	-35.33	530.84

Energies in kJ/mol.

Figure 6 shows the HOMO and LUMO patterns of the models considered. As seen in
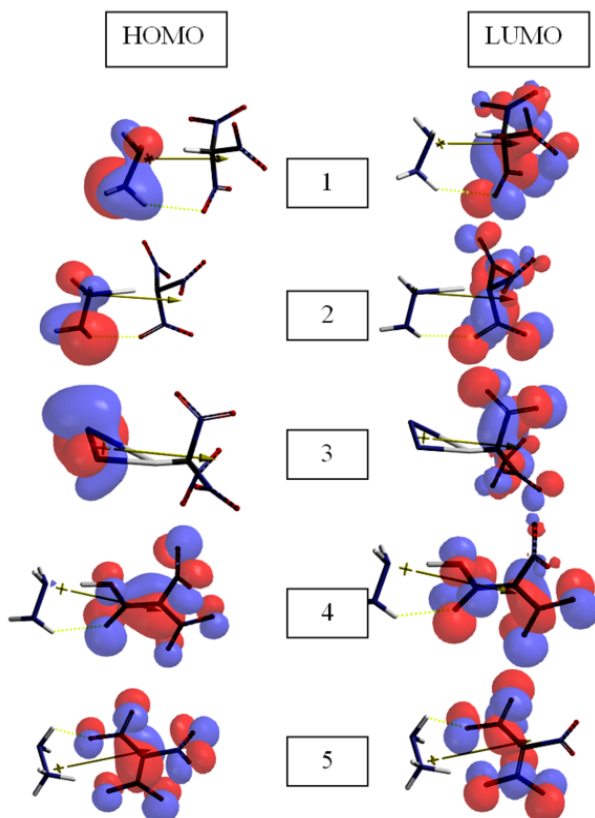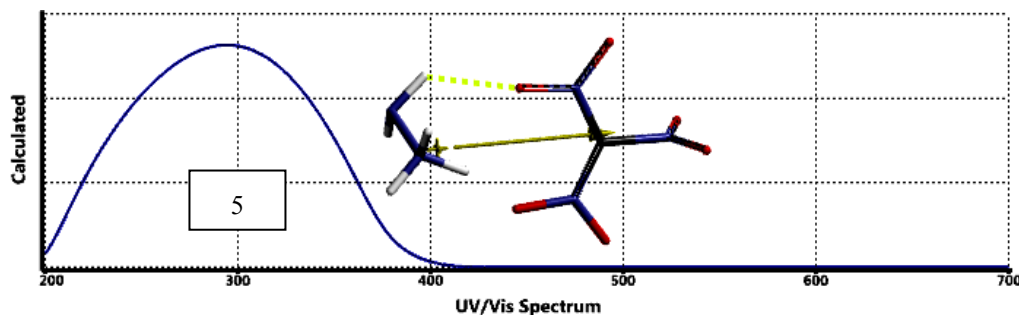

Figure 6. The HOMO and LUMO patterns of the models considered.

the figure, the nitroform moiety in figures 1-3 does not contribute to the HOMO. As for the LUMO, this time hydrazine does not contribute to the LUMO. In models 4 and 5 hydrazine neither contributes to the HOMO nor the LUMO.

Figure 7 is the calculated UV-VIS (time dependent density functional) spectra of the
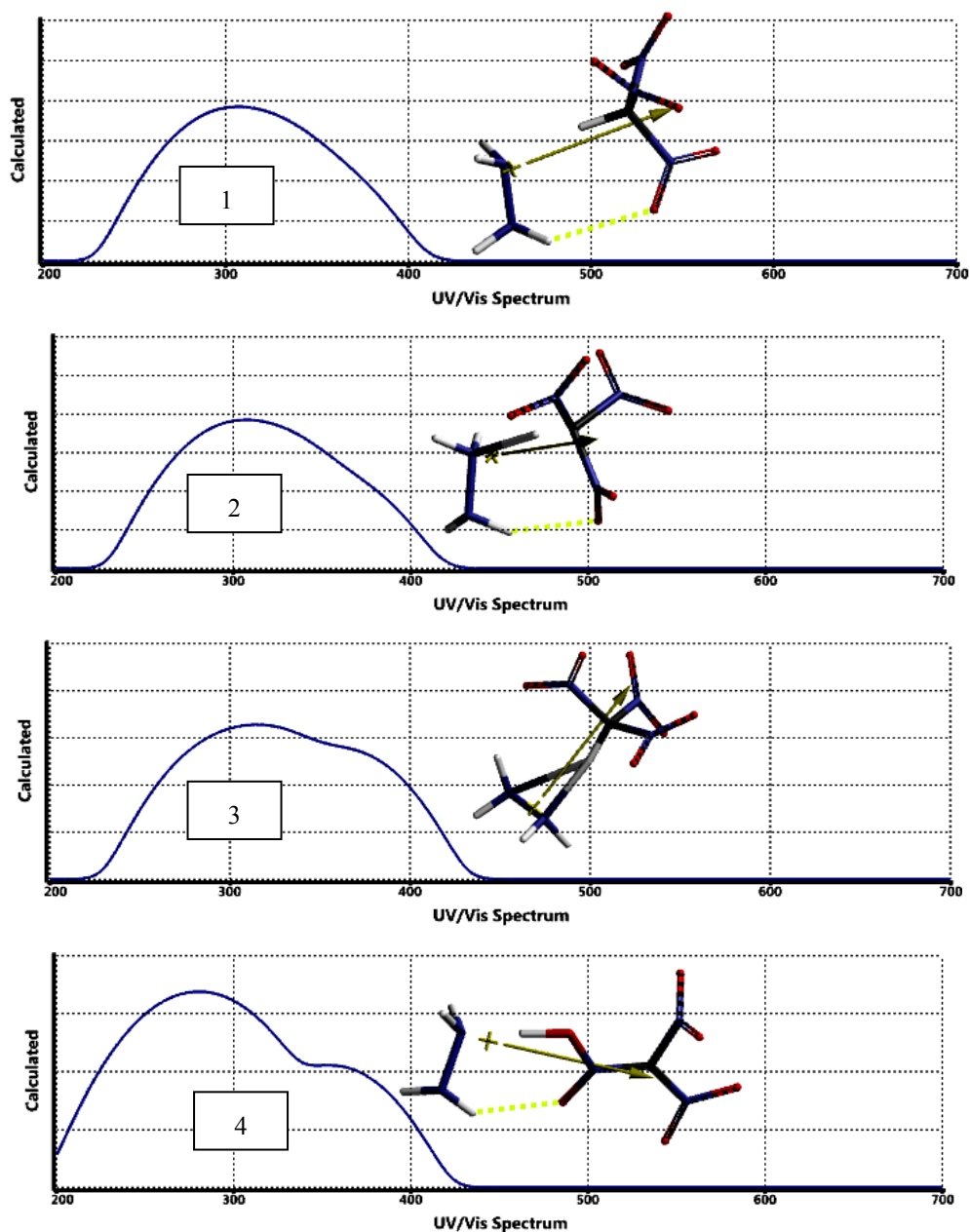
Figure 7. Calculated UV-VIS spectra of the models considered.

models considered. As seen in the spectrums, the perturbation caused by the nature of the models progressively disturbs the absorptions in models 1-4. Figure 8 is the calculated UV-VIS spectra of nitroform and the nitroformate ion. The spectra of the models mainly resemble the spectrum of nitroform. In the models or in the nitroformate ion due to some but little extended conjugation (and/or some other perturbations) a shoulder or a new λ_{max} value appears and a slight bathochromic effect is observed.
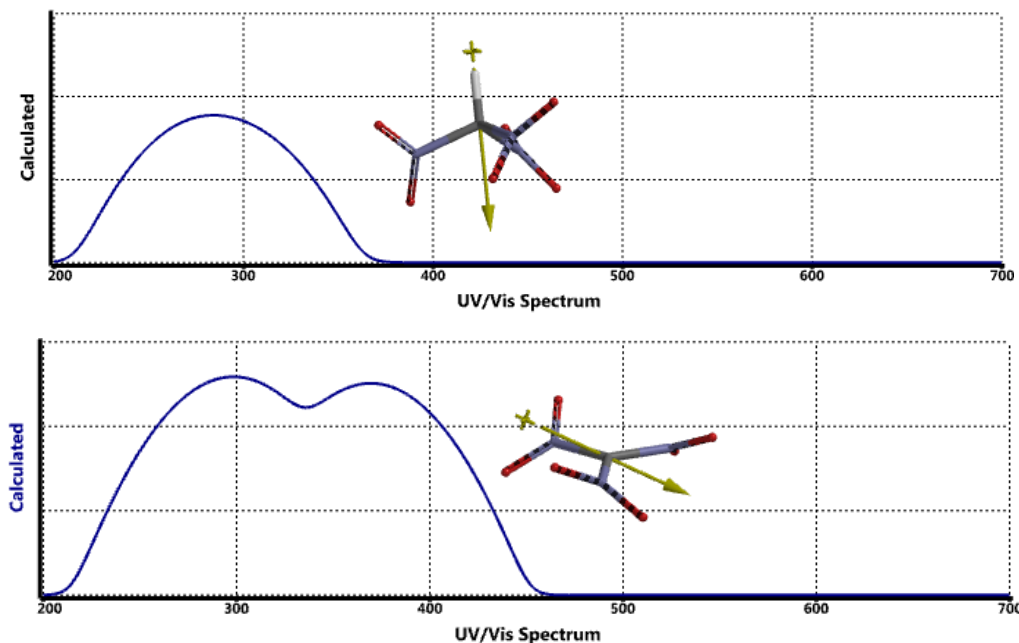
Figure 8. Calculated UV-VIS spectra of nitroform and nitroformate ion.

Note that within the constraints of the theory and the basis set employed the optimized structure of nitroformate anion, unlike to many carbane ions, is a planar structure with twisted nitro groups around it (like a carbonium ion) (see Figure 8).

4. Conclusion

The present density functional treatment, within the restrictions of the theory and the basis set employed, considers the interaction between hydrazine and nitroform via various models including ion pair formation and nitro and *aci* tautomeric forms of nitroform. The cyclic model seems to be the most stable of all. In models 1-3 which are more stable (electronically and thermodynamically) than the other models, hydrogen atom originating from nitroform is in the close proximity of the carbon atom rather than the vicinity of the hydrazine nitrogen atoms. Therefore, the interaction between the hydrazine and nitroform should be predominantly a nonbonding type.

References

[1] Schoyer, H.F.R., Welland-Veltman, W.H.M., Louwers, J., Korting, P.A.O.G., van der Heijden, A.E.D.M., Keizers, H.L.J., & van den Berg, R.P. (2002). Overview of the development of hydrazinium nitroformate. *Journal of Propulsion and Power*, *18*(1), 131-137. https://doi.org/10.2514/2.5908

[2] Dendage, P.S., Sarwade, D.B., Asthana, S.N., & Singh, H. (2001). Hydrazinium nitroformate (HNF) and HNF based propellants: A review, *Journal of Energetic Materials*, *19*(1), 41-78. https://doi.org/10.1080/07370650108219392

[3] Dickens, B. (1967). Crystal structure of hydrazine nitroform $[N_2H_5{}^+C(NO_2)_3{}^-]$, *Chemical Communications*, *5*, 246-247. https://doi.org/10.1039/C19670000246

[4] Ledgard, J. (2007). *The preparatory manual of explosives.* ISBN 9780615142906

[5] Du, L., Jin, S., Liu, Y., Wang, M., Li, J., Lan, G., Nie, P., & Li, L. (2019). Theoretical study on the weak interaction and energy performance of nitroformate salts and nitroformate-based propellant formulations, Journal of *Molecular Modeling*, *25*, 285, 1-10. https://doi.org/10.1007/s00894-019-4164-7

[6] Göbel, M., & Klapötke, T.M. (2007). Potassium-, ammonium-, hydrazinium-, guanidinium-, aminoguanidinium-, diaminoguanidinium-,triaminoguanidinium- and melaminium nitroformate – synthesis, characterization and energetic properties, *Z. Anorg. Allg. Chem*., *633*, 1006-1017. https://doi.org/10.1002/zaac.200700114

[7] Baxter, A.F., Martin, I., Christe, K.O., & Haiges, R. (2018). Formamidinium nitroformate: an insensitive RDX alternative, *J. Am. Chem. Soc. 140*, 15089-15098. https://doi.org/10.1021/jacs.8b10200

[8] Huang, Y., Gao, H., Twamley, B., & Shreeve, J.M. (2007). Synthesis and characterization of new energetic nitroformate salts, *Eur. J. Inorg. Chem*., *14*, 2025-2030. https://doi.org/10.1002/ejic.200601228

[9] Göbel, M., Klapötke, T.M., & Mayer, P. (2006). Crystal structures of the potassium and silver salts of nitroform, *Z. Anorg. Allg. Chem*., *632*, 1043-1050. https://doi.org/10.1002/zaac.200500525

[10] Yang, L., Zhang, J., Zhang, T., Zhang, J., & Cui, Y. (2009). Crystal structures, thermal decompositions and sensitivity properties of [Cu(ethylenediamine)$_2$(nitroformate)$_2$] and [Cd(ethylenediamine)$_3$] (nitroformate)$_2$, *J. Hazard. Mater*., *164*, 962-967. https://doi.org/10.1016/j.jhazmat.2008.08.096

[11] Bryan, J.C., Burnett, M.N., & Gakh, A.A. (1998). Tetrabutylammonium and caesium salts of trinitromethane, *Acta Cryst. C54*, 1229-1233. https://doi.org/10.1107/S0108270198004491

[12] Cioslowski, J., Mixon, S.T., & Fleischmann, E.D. (1991). Electronic structures of trifluoro-, tricyano-, and trinitromethane and their conjugate bases, *J. Am. Chem. Soc. 113*, 4751-4755. https://doi.org/10.1021/ja00013a007

[13] Ju, X-H., Xiao, J-J., & Xiao, H-M. (2003). DFT Study of the intermolecular interaction of hydrazinium nitroformate ion pair, *Chemical Journal of Chinese Universities*, *24*(6), 1067-1071. http://www.cjcu.jlu.edu.cn/CN/Y2003/V24/I6/1067

[14] Urbanski, T. (1984). *Chemistry and technology of explosives* (Vol. 4)*.* Oxford: Pergamon, UK. https://doi.org/10.1002/ijch.196400070

[15] Jones, J.R. (1972). The ionization of carbon acids, In *Annual Reports on the Progress of Chemistry, Section A: General Physical and Inorganic Chemistry* (Ch.5, Vol. 69, pp. 119-132). London: Academic.

[16] Murray, J.S., Lane, P., Göbel, M., Klapötke, T.M., & Politzer, P. (2009). Intra- and intermolecular electrostatic interactions and their significance for the structure, acidity, and tautomerization behavior of trinitromethane, *The Journal of Chemical Physics*, *130*, 104304. https://doi.org/10.1063/1.3082406

[17] Stewart, J.J.P. (1989). Optimization of parameters for semiempirical methods I. Method. *J. Comput. Chem*., *10*, 209-220. https://doi.org/10.1002/jcc.540100208

[18] Stewart, J.J.P. (1989). Optimization of parameters for semiempirical methods II. Application. *J. Comput. Chem*., *10*, 221-264. https://doi.org/10.1002/jcc.540100209

[19] Leach, A.R. (1997). *Molecular modeling*. Essex: Longman.

[20] Fletcher, P. (1990). *Practical methods of optimization*. New York: Wiley.

[21] Kohn, W., & Sham, L. (1965). Self-consistent equations including exchange and correlation effects. *J. Phys. Rev.*, *140*, A1133-A1138. https://doi.org/10.1103/PhysRev.140.A1133

[22] Parr R.G., & Yang, W. (1989). *Density functional theory of atoms and molecules*. London: Oxford University Press.

[23] Cramer, C.J. (2004). *Essentials of computational chemistry*. Chichester, West Sussex: Wiley.

[24] Becke, A.D. (1988). Density-functional exchange-energy approximation with correct asymptotic behavior. *Phys. Rev. A*, *38*, 3098-3100. https://doi.org/10.1103/PhysRevA.38.3098

[25] Vosko, S.H., Wilk, L., & Nusair, M. (1980). Accurate spin-dependent electron liquid correlation energies for local spin density calculations: a critical analysis. *Can. J. Phys.*, *58*, 1200-1211. https://doi.org/10.1139/p80-159

[26] Lee, C., Yang, W., & Parr, R.G. (1988). Development of the Colle-Salvetti correlation energy formula into a functional of the electron density. *Phys. Rev. B*, *37*, 785-789. https://doi.org/10.1103/PhysRevB.37.785

[27] SPARTAN 06 (2006). Wavefunction Inc., Irvine CA, USA.